Research Article **Open Access**

Jasim M. Abbas*, Zamri Chik, Mohd Raihan Taha

Modelling and Assessment of a Single Pile Subjected to Lateral Load

https://doi.org/10.2478/sgem-2018-0009
received December 14, 2017; accepted March 23, 2018.

Abstract: A three-dimensional finite element technique was used to analyse single pile lateral response subjected to pure lateral load. The main objective of this study is to assess the influence of the pile slenderness ratio on the lateral behaviour of single pile. The lateral single pile response in this assessment considered both lateral pile displacement and lateral soil resistance. As a result, modified p-y curves for lateral single pile response were improved when taking into account the influence lateral load magnitudes, pile cross sectional shape and flexural rigidity of the pile. The finite element method includes linear elastic, Mohr-Coulomb and 16-nodes interface models to represent the pile behaviour, soil performance and interface element, respectively. It can be concluded that the lateral pile deformation and lateral soil resistance because of the lateral load are always influenced by lateral load intensity and soil type as well as a pile slenderness ratio (*L/D*). The pile under an intermediate and large amount of loading (in case of cohesionless soil) has more resistance (low lateral displacement) than the pile embedded on the cohesion soil. In addition, it can be observed that the square-shaped pile is able to resist the load by about 30% more than the circular pile. On the other hand, pile in cohesionless soil was less affected by the change in *EI* compared with that in cohesive soil.

Keywords: piles; lateral response; slenderness ratio; flexural rigidity; 3D FE analysis.

1 Introduction

In the design of pile subjected to lateral load, the lateral displacement at working loads should be within the permissible limit [18,20,22]. In addition, the second main key element in the design of laterally loaded piles is the determination of ultimate lateral resistance that can be exerted by soil against the pile [25], particularly the ultimate soil pressure which occurred in the middle of the pile.

The performance of piles when subjected to lateral loads is responsive to soil properties in the upper part of soil layer [6,7]. As the surface layers may be subject to disturbance, practically, traditional soil parameters should be adopted in the calculation of lateral pile displacement. In the case of piles under lateral loading, the failure criterion of short piles under lateral loads when compared to those of long piles varies and unlike the design procedure is suitable. Therefore, studying the effect of slenderness on the lateral single isolated pile response is important and still needs more assessment.

From Figure 1, t can be observed that the pile in case of short pile failure criteria and free head condition failed by full pile rotation around the point near to the pile base. Whilst in case of fixed head, the pile maybe fully moved and, at the same time, with small rotation near to the pile base. On the other hand, the long pile failure occurs near to the pile head by pile fracture and keeps the other embedded length without failure. In the case of fixed head long pile, the failure occurred at the fracture point as well as pile cap [6,7]. Real pile behaviour generally falls somewhere between the free- and fixed-head conditions because a small rotation of the pile head is expected, even when the pile is connected to a cap [17].

Many researches have also been performed to study the response of laterally loaded piles in different types of soil. A preliminary survey of the literatures available on this topic was given by [6,7,14], but little knowledge was received regarding the influence of the pile slenderness ratio on the lateral pile response, in addition to the

***Corresponding author: Jasim M. Abbas,** Department of Civil Engineering, College of Engineering, University of Diyala, Iraq, E-mail: jasimalshamary@yahoo.ccom
Zamri Chik, Mohd Raihan Taha: Department of Civil and Structural Engineering, Universiti Kebangsaan Malaysia

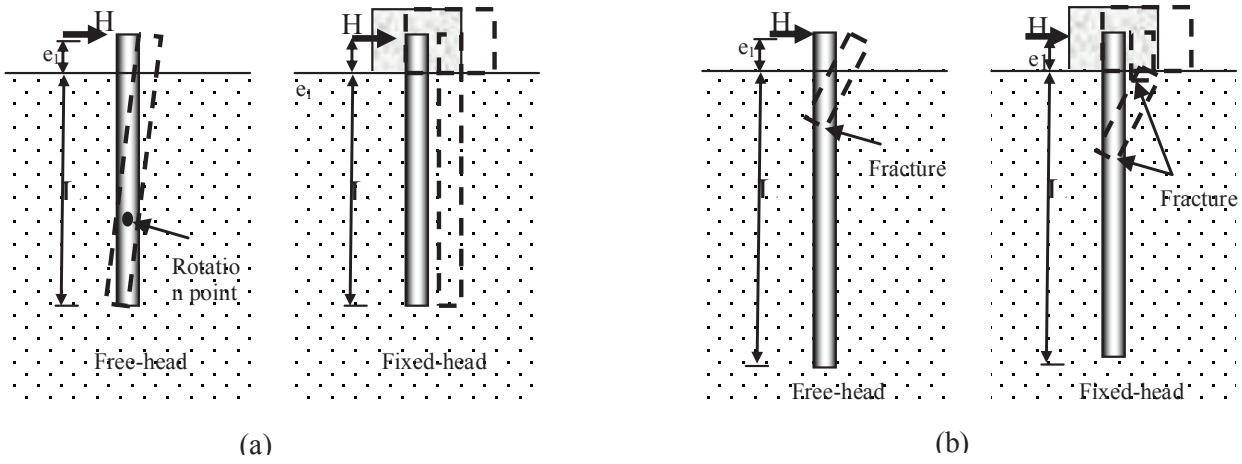

Figure 1: Failure modes of vertical pile under lateral load (Broms, 1964a&b): (a) short pile under lateral load and (b) long pile under lateral load.

influence of lateral load magnitudes, cross sectional shape of the pile and flexural rigidity of the pile.

It is generally accepted that the finite element method is the major technique used in numerical analysis of geotechnical problems, particularly piles and soil consolidation. As reported by [20], the first attempt to study the lateral behaviour of piles includes a two-dimensional (2D) finite element model in the horizontal plane. Anagnostopoulos and Georgiadis (1992) attempted to explain the lateral pile response through an experimental model supported by a 2D finite element analysis. Other investigations have attempted to study the lateral response of pile under pure lateral load using the finite element approach [9,11,16,23,24]. In addition, the influence the lateral pile response in 3D finite element approach when the pile carried both axial and lateral loads was studied by [12,13] and [1,2].

Therefore, in this study, the importance of conducting a fundamental study is discussed. A fundamental study of the lateral pile response under pure lateral load was conducted by varying a simulation parameter of the pile material (i.e. the geometric dimension of the pile such as slenderness ratio, *D*, flexural rigidity of the pile, *EI*) and soil properties (i.e. cohesionless soil and cohesive soil).

2 Analysis Methodology and Layout

Finite element analyses were performed using the software PLAXIS 3D Foundation. In the finite element method, a continuum is divided into a number of (volume) elements. Each element consists of a number of nodes. Each node has a number of degrees of freedom that correspond to discrete values of the unknowns in the boundary value problem to be solved. The finite element mesh used in the simulation of single pile analysis (shown in Fig. 2) consists of 15-nodes wedge element (1,134), including (1,099) soil element and (35) pile elements. The lateral load is applied at the tip of the pile that is found on the ground surface in the x-direction and at y-direction when axial loads are applied. Plain and 3D view for the finite element mesh of single pile and surrounded the soil mass is given in Figure 2. The outer boundaries of soil body of cubic shape are extended to 10D on the sides and 5D at the bottom of pile base.

Analyses were performed with several trail meshes with increasing mesh refinement until the displacement changes to very minimal with more refinement. The aspect ratio of elements used in the mesh is small and closed to the pile body near to the pile top and base. All the nodes of the lateral boundaries (right and bottom) are restrained from moving in the normal direction to the respective surface.

The finite element simulation includes the following constitutive relationships for pile, surrounded soil and interface element. The finite element includes a linear elastic model to simulate structural part of the problem (e.g. pile), Mohr-Coulomb model to represent the surrounded soil and 16-node interface elements to represent an interface element. These constitutive models are illustrated as follows:

*Structural Members Model***:** The use of the linear elastic model is quite common to model massive structures in the soil or bedrock layers that include piles and so on [5]. This model represents Hooke's law of isotropic linear elasticity used for modeiling the stress–strain relationship of the pile material. The model involves two elastic stiffness parameters, namely, the effective Young's modulus, *E*', and the effective Poisson's ratio, *v*'.

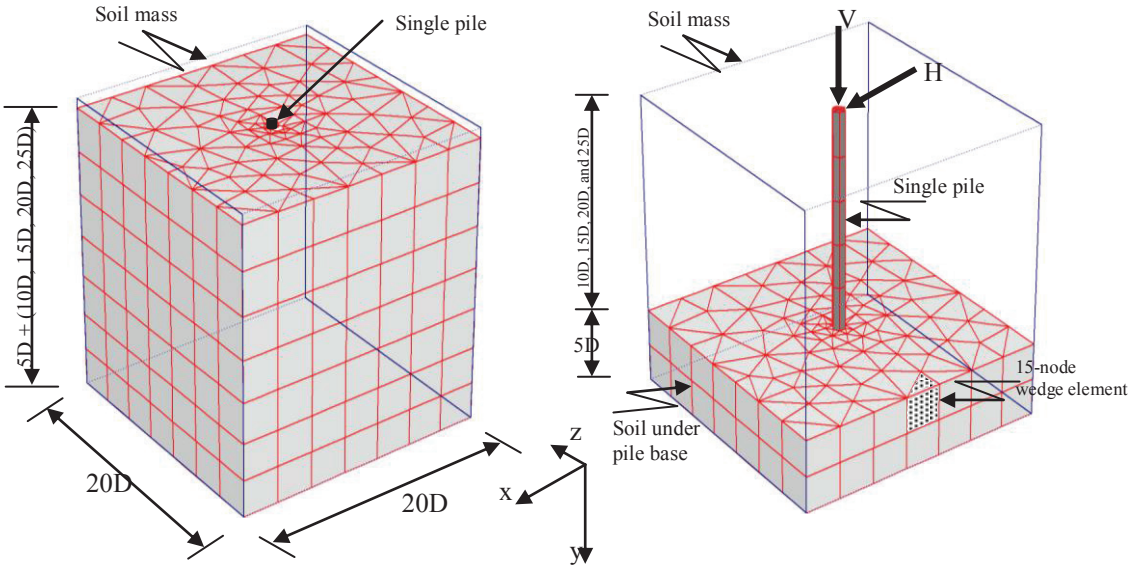

Figure 2: Three dimension of finite element mash for single pile and surrounded soil mass,

Soil Model: The surrounding soil is represented by Mohr–Coulomb's model. This elasto-plastic model is based on soil parameters that are known in most practical situations. The model involves two main parameters, namely, the cohesion intercept, *c'*, and the friction angle, *f'*. In addition, three parametersnamely, Young's modulus, *E'*; Poisson's ratio, *v'*; and the dilatancy angle, *ψ'* – are needed to calculate the complete stress-strain (σ, *e*) behaviour. The failure envelope as referred by [21] and [9] only depends on the principal stresses (σ_1', σ_3') and is independent of the intermediate principle stress (σ_2').

Interface Elements Model: Interfaces are modeiled as 16-node interface elements. Interface elements consist of eight pairs of nodes, compatible with the eight-noded quadrilateral side of a soil element. Along the degenerated soil elements, interface elements are composed of six-node pairs, compatible with the triangular side of the degenerated soil element. Each interface has a *virtual thickness* assigned to it, which is an imaginary dimension used to obtain the stiffness properties of the interface. The virtual thickness is defined as the virtual thickness factor multiplied by the average element size.

3 Validation of numerical model

This section used to assess the accuracy of the finite element approach in analysing laterally loaded piles and to verify certain details of the finite element such as pile displacement. The comparative case includes full-scale lateral load tests reported by [10]. The results of laboratory and field tests are used to identify the soil profiles and soil properties that are well instrumented.

The case study deals with lateral load in which the deflection response of bored piles in cemented sand was examined by field test on a single pile under lateral load [10]. All piles were 0.3 m in diameter and had a length of 3 or 5m. The site of this load test was in Kuwait. The soil profile consists of a medium dense cemented silty sand layer to a depth of 3 m. This is underlain by a medium dense to very dense silty sand with cemented lumps to the bottom of the borehole. The same load sequence as pile tests was applied to the pile after completing the whole geotechnical model for lateral pile tests. The properties of soil in the both cases are listed in Table 1.

The comparison between the finite element results and field test data is shown in Figure 3. The numerical simulation is reasonably accurate for the problem of laterally loaded piles and pile-soil interaction over a wide range of deformation for 3 and 5m long piles. The pile with a length of 5m is highly resistance to the lateral load from the second pile length value. Comparable data were obtained between the experimental results of the three piles and the present simulation model. The results obtained from the numerical simulation for a pile of 5 m is relatively closed with the results obtained from the field test. Whilst the result from the numerical simulation is not too closed in case of 3-m long pile, it may be due to non-homogeneous soil around the pile in field.

Table 1: Geotechnical properties of the soil layers.

	Saturated soil weight (kN/m³)	Young's modulus (kPa)	Poisson's ratio	Cohesion intercept (kPa)	Friction angle
Medium dense cemented silty sand layer	18	1.3x104	0.3	20	35
Medium dense to very dense silty sand with cemented lumps	19	1.3 x104	0.3	1	45
Pile	-	2.0 x109	0.15	-	-

Table 2: Soil parameters for analysis of pile group.

Parameters	Unit	Cohesionless soil	Cohesive soil
Unit weight, γ'	kN/m³	20.0	18.0
Young's modulus, E'	MPa	1.3×10^4	1.0×10^4
Poisson's ratio, v'	-	0.3	0.35
Cohesion intercept, c'	MPa	0.1	5.0
Angle of internal friction, ϕ'	-	30	25

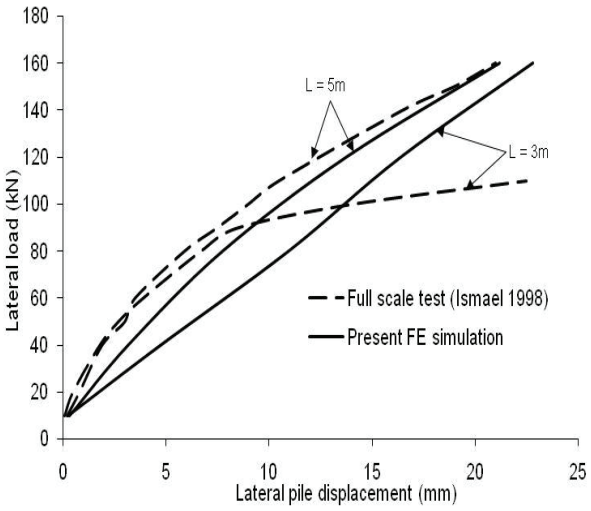

Figure 3: Comparison of finite element results with field test data of Ismael (1998).

4 Result and Discussion

The study includes the lateral pile response (i.e. lateral pile displacement and lateral soil pressure) under pure lateral load. Two types of soil were used (i.e. cohesionless and cohesive soils). Lateral load intensity H ranged (5-45) $\{\gamma_w D^3\}$. Slenderness ratio, L/D, was 10, 15, 20 and 25. Pile shape and soil type (cohesionless soil and cohesive soil) are detailed in this section. The baseline soil parameters used for the analysis of laterally loaded pile group are illustrated in Table 2.

4.1 Influence of lateral load intensities

The lateral pile deformation and lateral soil resistance because of the lateral load are always influenced by the lateral load intensity and soil type as well as a pile slenderness ratio (L/B). Figure 4 presents the effect of lateral load intensity and soil type on the deformation behaviour of pile along the pile length for four pile slenderness ratio under lateral load show circular pile: (a) the short pile (L/B = 10) gives a small amount of lateral tip deflection for the same amount of loading than the piles that have the slenderness ratio more than 10; (b) the deflection along the pile is always in the direction of load (assumed negative). These values change to positive and pass through zero, depending on the slenderness ratio. For the short pile (L/D = 10), the point of inflection is 1/5 from the base of the pile, whilst for the long pile (L/D = 15) and (L/D = 20), the point position is (1/2)L and (3/5)L from the base, respectively. Finally, for the long pile (L/D = 25), the point of inflection (fracture point) is (7/10)L from the base. This is due to the slenderness of the pile that carry the load along the pile length in the case of short piles, but the upper part of pile carry applied load in the case of long piles. In the case of short pile, the pile body tends to rotate around the inflection point and produce a small negative deflection closed to the pile base. The negative deflection occurred in the opposite direction of the load. The maximum negative deflection occurred exactly at the base of the pile.

In general, the lateral pile responded closely in cases of both cohesionless and cohesive soils when small amounts of loading were applied to all cases of slenderness ratio. As shown in the results, the pile under low and a large amount of loading (in the case of cohesionless soil) presented more resistance (low lateral displacement) than the pile embedded in the cohesion soil. This is possibly due to high soil stiffness.

Lateral soil pressure (p) in soil resulting from the lateral loads is shown in Figure 4. It can be observed that the pressure increased with depth. Higher values of pressure occurred in the position of L/D between 6 and 8

when lateral loads of 250 and 450 kN were applied. Also at L/D = 2, which is the point of rotation, near the values of lateral soil pressure can be observed. As a conclusion from the results, the pile in cohesionless soil is less safe against ultimate soil pressure failure and has less resistance against lateral pile displacement failure. The location (zero lateral pressure) was also indicted [6,12,13] who respectively studied only on pure lateral load (no vertical load) and with the application of axial loads. Thus, the position of the maximum lateral soil pressure changes with vertical load intensity.

The influence of the pile slenderness ratio on the lateral pile tip displacement is assessed by fixed pile diameter and increase in the pile length (i.e. L = 10, 15, 20 and 25 m). During this study, the soil and pile parameters were kept unchanged. The influence of the pile slenderness ratio L/D on the lateral pile tip displacement is presented in Figure 5. The study compared both types of soil under three load intensities (i.e. 50, 250 and 450kN). At the low load magnitude, very little changes were observed in the lateral pile displacement with respect to the pile slenderness ratios for both cohesionless and cohesive soils. Whilst the displacement at the loads 250 and 450 kN increased to 20% and 35%, respectively.

The p-y curve predicted from finite element at two depths (z=0 and z=L/5D from ground surface) for both cohesionless and cohesive soils is shown in Figure 6. The initial values of the computed p-y curves are insensitive to the soil type and pile diameter. The result from this is closed to the assumption by Fan and Long (2005). From this figure, it can be observed that the behaviour of p–y curves was non-linear which results from the non-linear relationship of ultimate lateral soil pressure with respect to pile slenderness ratio; this also supported the assumption [25] and unsupported the assumption proposed [6,7], which observed linear relation of the ultimate lateral soil pressure with respect to pile slenderness ratio.

4.2 Influence of pile shape

One of the main advantages of the 3D finite element simulation is the personification of the shape effect. The previous investigations show that the response of pile to lateral load is moderately affected by the shape of cross section [15]. Therefore, this study includes mainly the effect of pile shape on the lateral pile response on both cohesionless and cohesive soils.

The lateral pile displacement of two pile shapes is shown in Figure 7, which detailed the increase in lateral deflection response with an increased amount of loading. Pile deflection change depends on the pile load increment. In the first stage of load, the pile response was uniform, which means that the pile deflection improves linearly. But the square-shaped pile shows more resistance than a circular pile, because of the high contact surface area between the pile and surrounding soil.

The results (Fig. 7) show distribution of the soil resistance along the pile depth under 450 kN load for two types of soil. As concluded from this and the previous section, the soil resistance for different pile shapes does not significantly change at low load level. It can be observed that the cross section of square-shaped pile has high amount of lateral soil pressure than those observed from the circular pile. This happened possibly due to a large contact surface area of the square-shaped pile compared with the circular pile. This assumption is supported by [15].

The maximum tip deflections of two shapes of pile are detailed in Figure 8. In general, for the low values of load, the lateral pile response was closed for the cross section of two shapes of pile and always near to the linear behaviour. Whilst, at higher loads, the piles behaved non-uniformly resulting from the non-linear response of soil around the pile, and this is supported [9]. From these results, it was mainly observed that the square-shaped pile is able to resist the load by about 30% more than the circular pile.

The p–y curve predicted from finite element at two depth (z=0 and z=L/5D) for both cohesionless and cohesive soils is shown in Figure 9. The p–y curves were predicted for two shapes of the pile (i.e. square shaped and circular). From this figure, it can be observed that different behaviours of pile with different shapes translate into different design values, if necessary, to design pile under lateral load. Therefore, it can be concluded that the pile is more sensitive to the pile shape as well as pile slenderness ratio.

4.3 Influence of flexural rigidity (*EI*)

In this study, the flexural rigidity (EI) change in three magnitudes was analysed; the values of EI were calculated by choosing various value of modulus of elasticity E and by keeping the magnitude of the moment of inertia I constant. The effect of the EI on the lateral pile displacement, lateral soil pressure and corresponding p–y curve illustrated are discussed in this section. The pile slenderness ratios (L/D) are 10, 15, 20 and 25. The behaviours of lateral pile displacement with pile depth for two types of soil are given in Figures 10 and 11. For lateral load of 450 kN at the pile tip, the lateral pile displacement

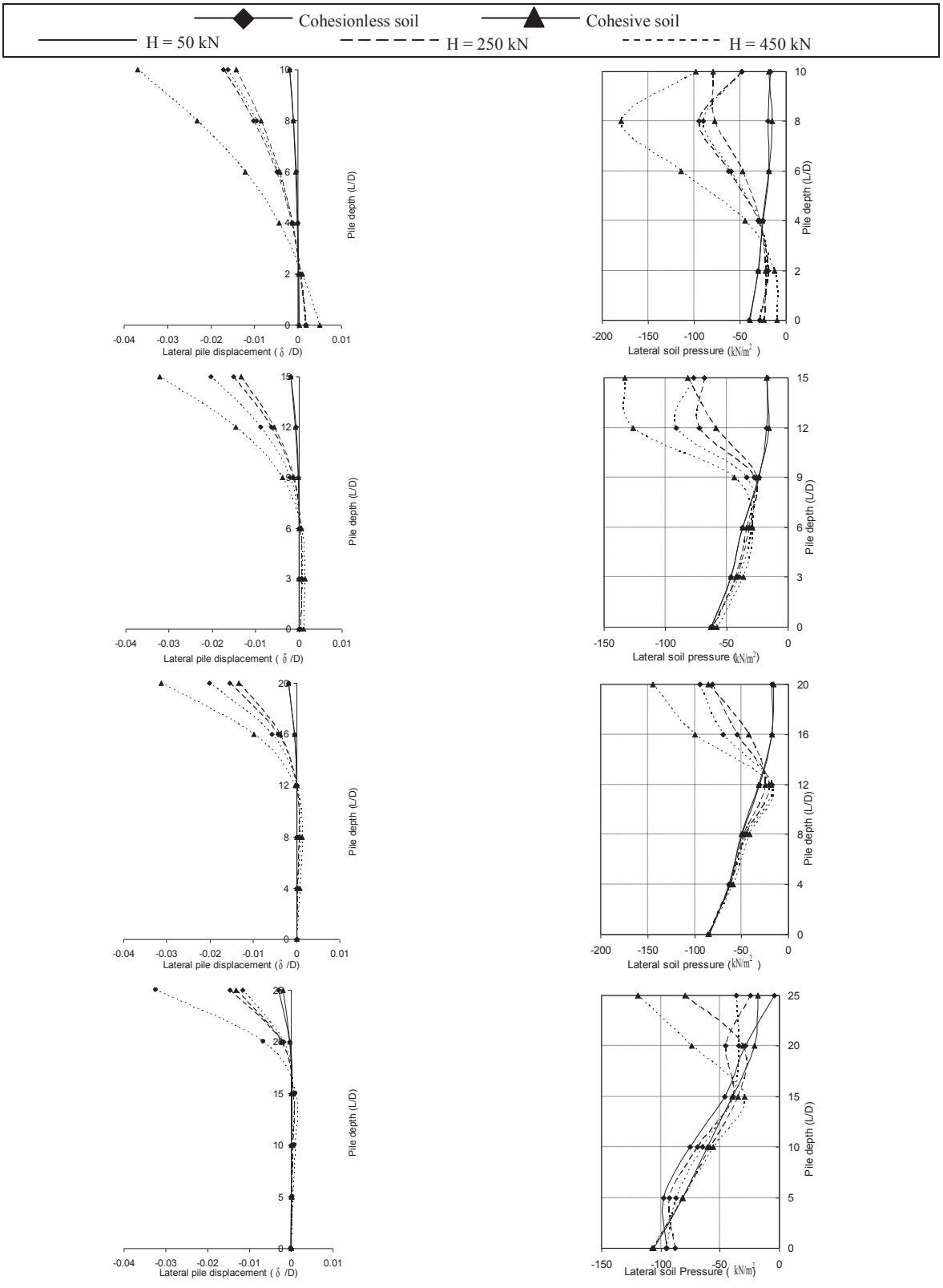

Figure 4: Influence of lateral load intensities on the lateral soil pressure distribution of pile embedded on both cohesionless and cohesive soils: (a) L = 10m, (b) L=15m, (c) L = 20 m and (d) L = 25 m.

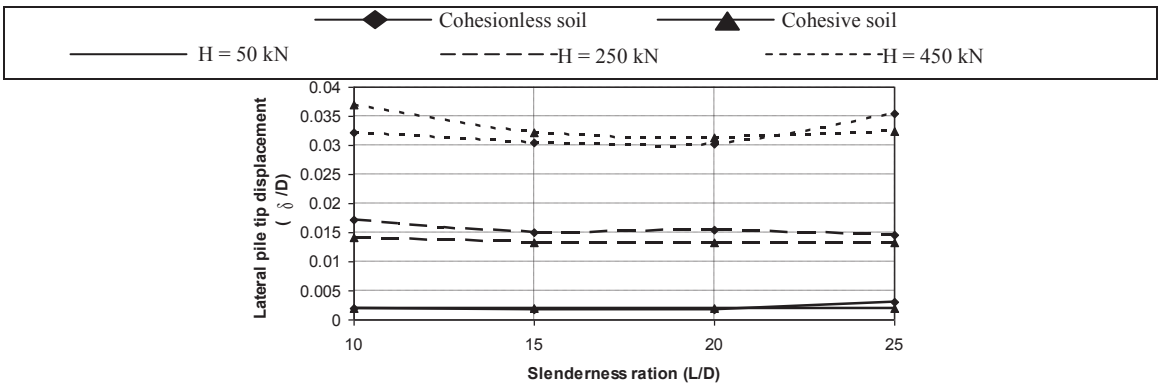

Figure 5: Predicted lateral tip displacement versus pile slenderness ratio under the influence of lateral load intensities.

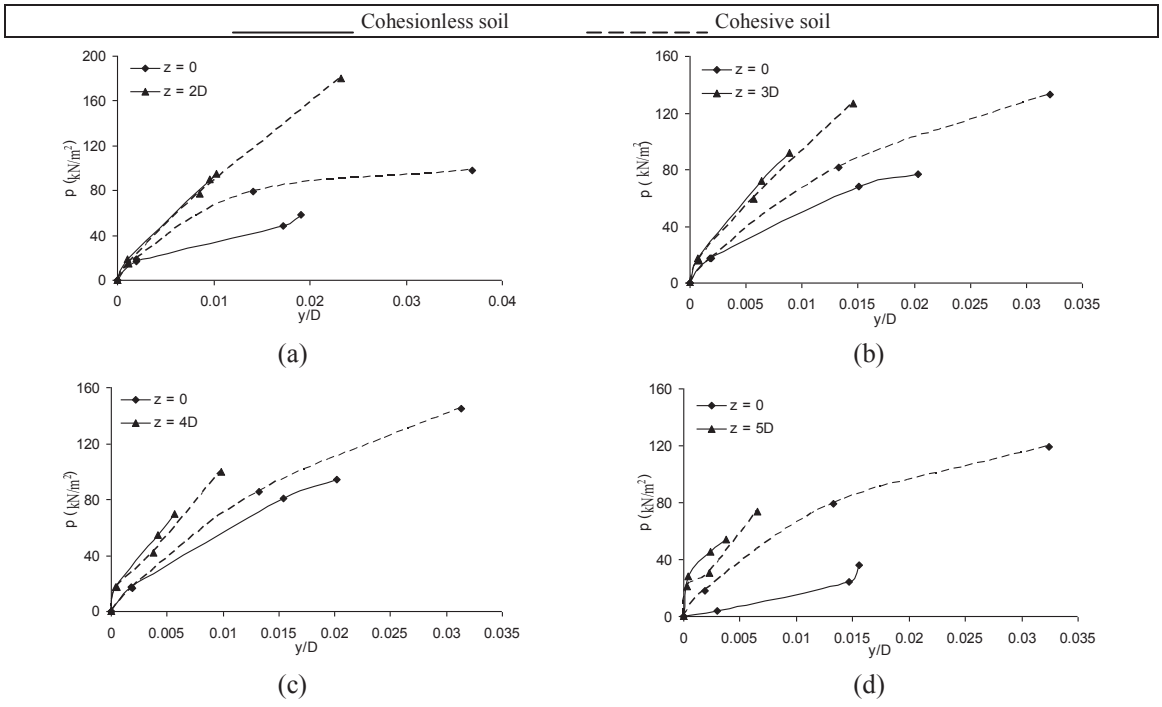

Figure 6: *p-y* curves predicted under the effect of lateral load intensities and pile slenderness ratio: (a) L = 10 m, (b) L = 15 m, (c) L = 20 m and (d) L = 25 m.

for *EI* magnitudes of *EI*= 1.4 × 105 kN m^2, *EI* = 1.4 × 106 kN m^2 and *EI* = 1.4 × 106 kN m^2. It can be observed that an increase in lateral pile displacement occurred when there is a decrease in pile flexural rigidity *EI*. It can also be observed that the pile with low amount of *EI* (e.g. 1.4 × 105 kN m^2) behave as a most flexible element, whilst, the pile with high amount of *EI* (e.g. 1.4 × 107 kN m^2) tend to behave as rigid element. The pile in cohesionless soil can also be seen as less affected by the change in *EI* compared with that in cohesive soil. For example, increase in lateral pile displacement in cohesionless soil was around 30–50% between lowest and highest *EI*, whilst the values were more than 70% in the case of pile in cohesive soil. Thus the pile in cohesionless soil is safer regarding the change in *EI* than that in cohesive soil.

The distribution of lateral soil resistance with pile depth embedded on two types of soil is illustrated in Figures 10 and 11. For the same lateral load condition, the pile with low value of *EI* (first case) deflects higher and more critical than the pile having high amount of *EI* (second case). Therefore, the pile in the first case receives more soil pressure than the pile in the second case.

The influence of the pile slenderness ratio *L/D* on the lateral pile tip displacement is shown in Figure 12.

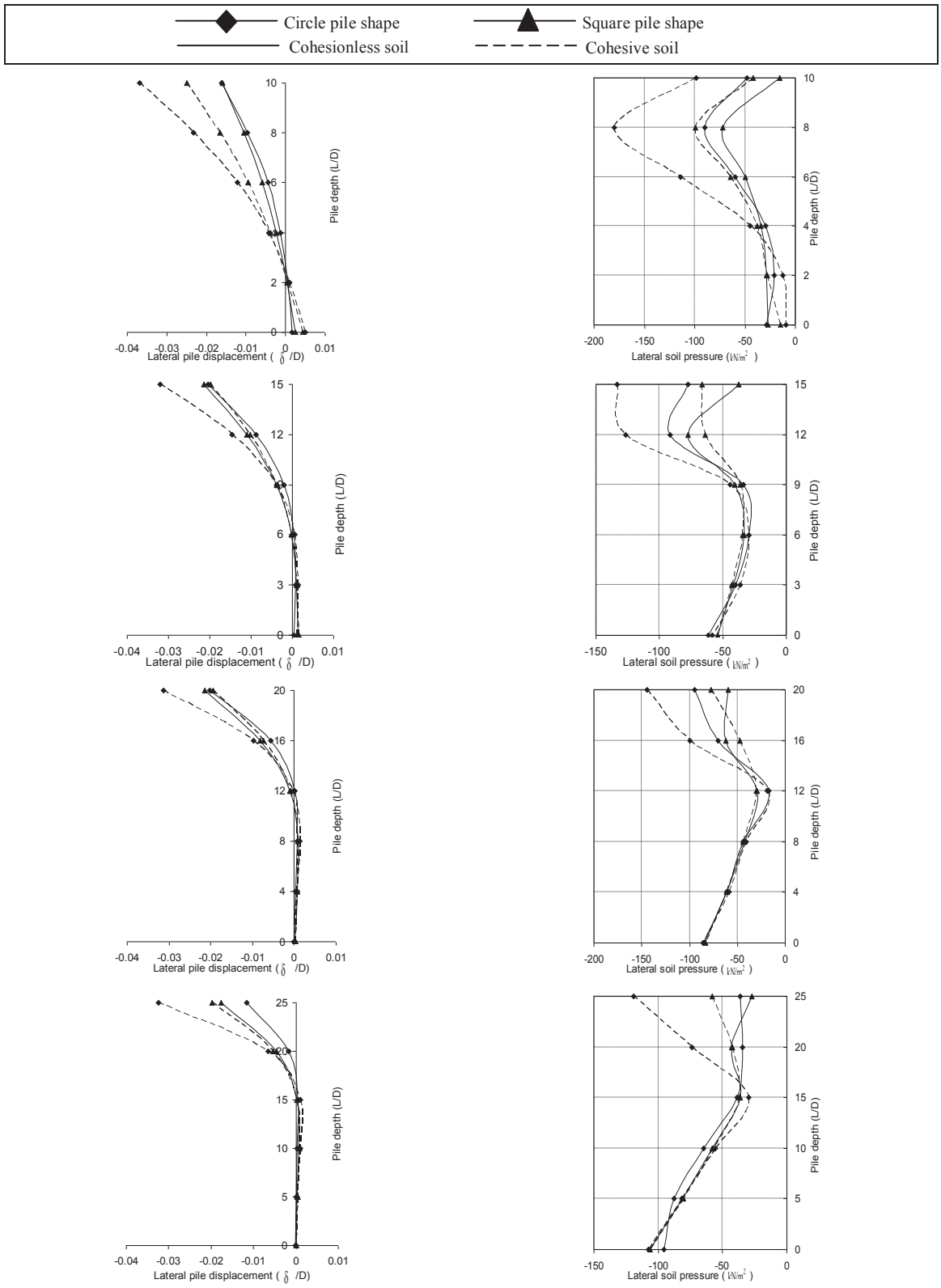

Figure 7: Influence of pile shape on the lateral soil pressure distribution of pile embedded on both cohesionless and cohesive soils: (a) L = 10 m, (b) L = 15 m, (c) L = 20 m and (d) L =25 m.

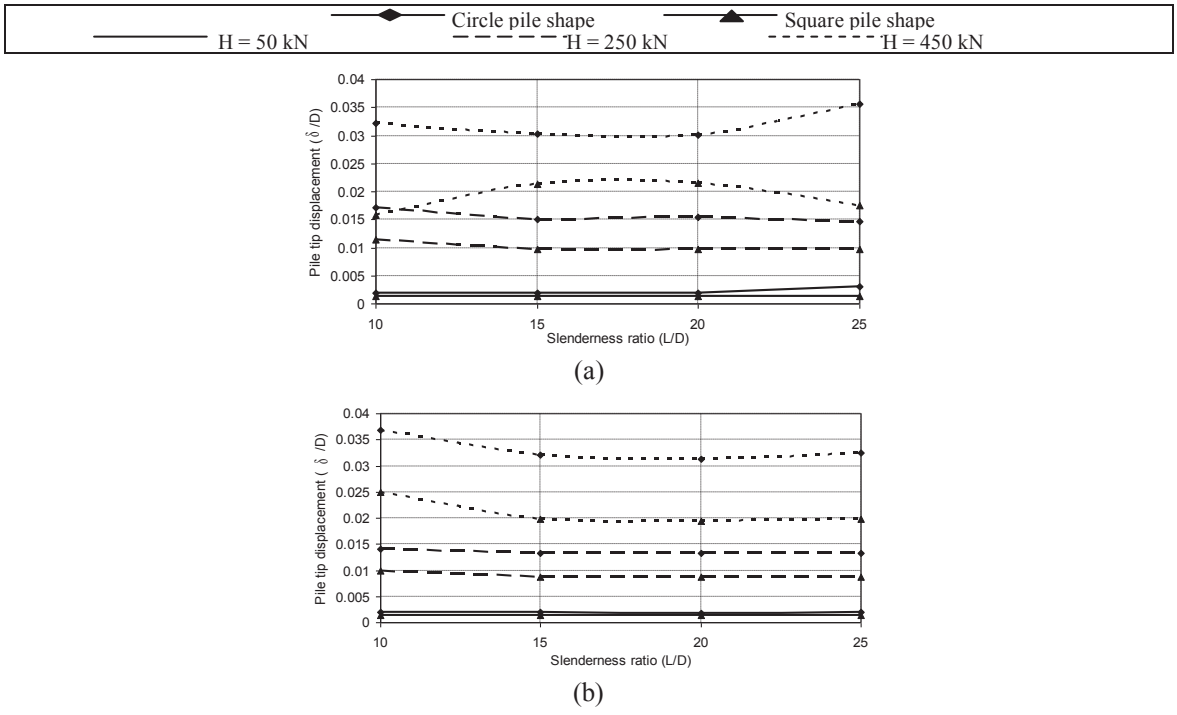

Figure 8: Predicted lateral tip displacement versus pile slenderness ratio under the influence of lateral load intensities and pile shape: (a) cohesionless soil and (b) cohesive soil

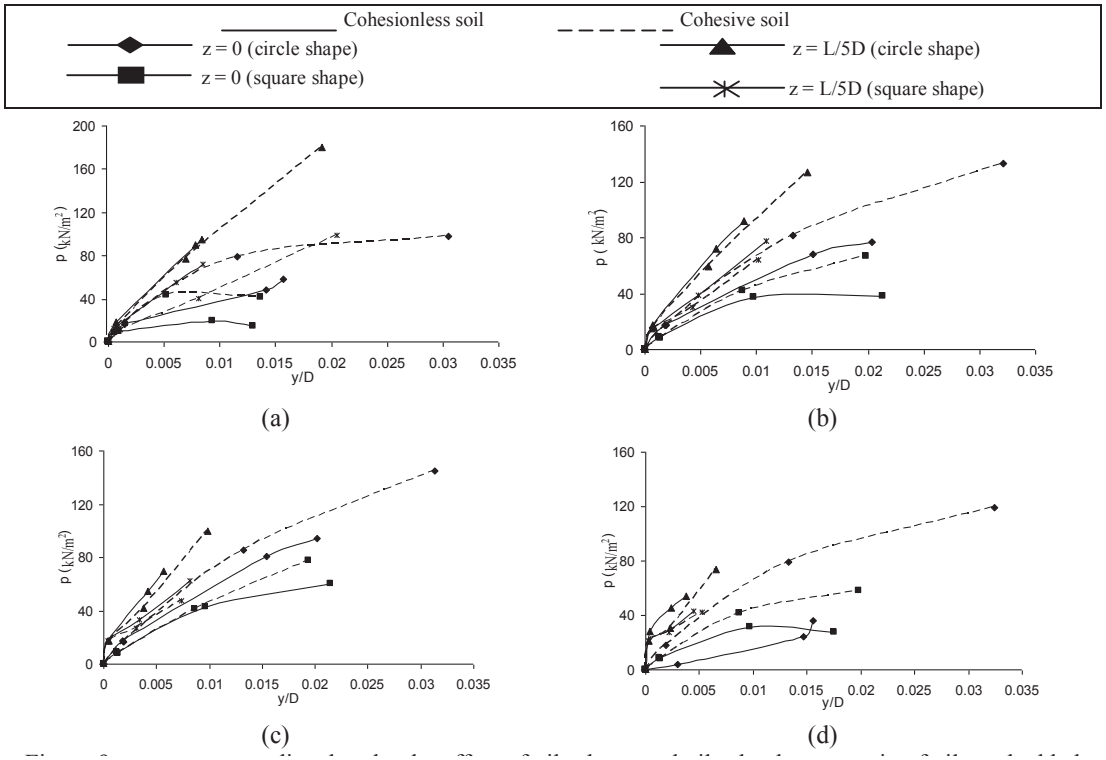

Figure 9: *p–y* curves predicted under the effect of pile shape and pile slenderness ratio of pile embedded on both cohesionless and cohesive soils: (a) $L/D = 10$, (b) $L/D = 15$, (c) $L/D = 20$ and (d) $L/D = 25$.

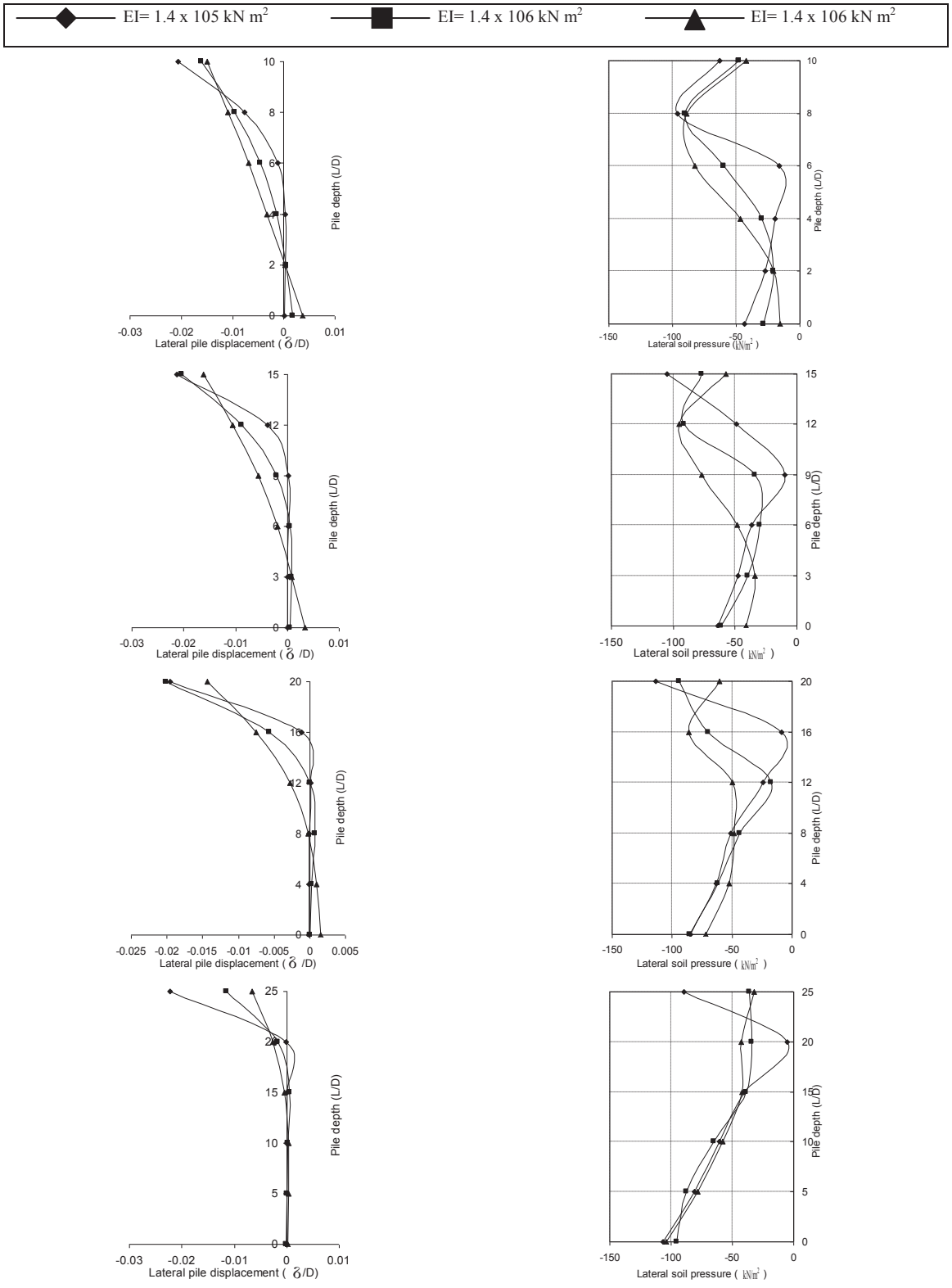

Figure 10: Influence of pile stiffness, *EI*, on the lateral soil pressure for cohesionless soil, (a) $L/D = 10$, (b) $L/D = 15$, (c) $L/D = 20$ and (d) $L/D = 25$.

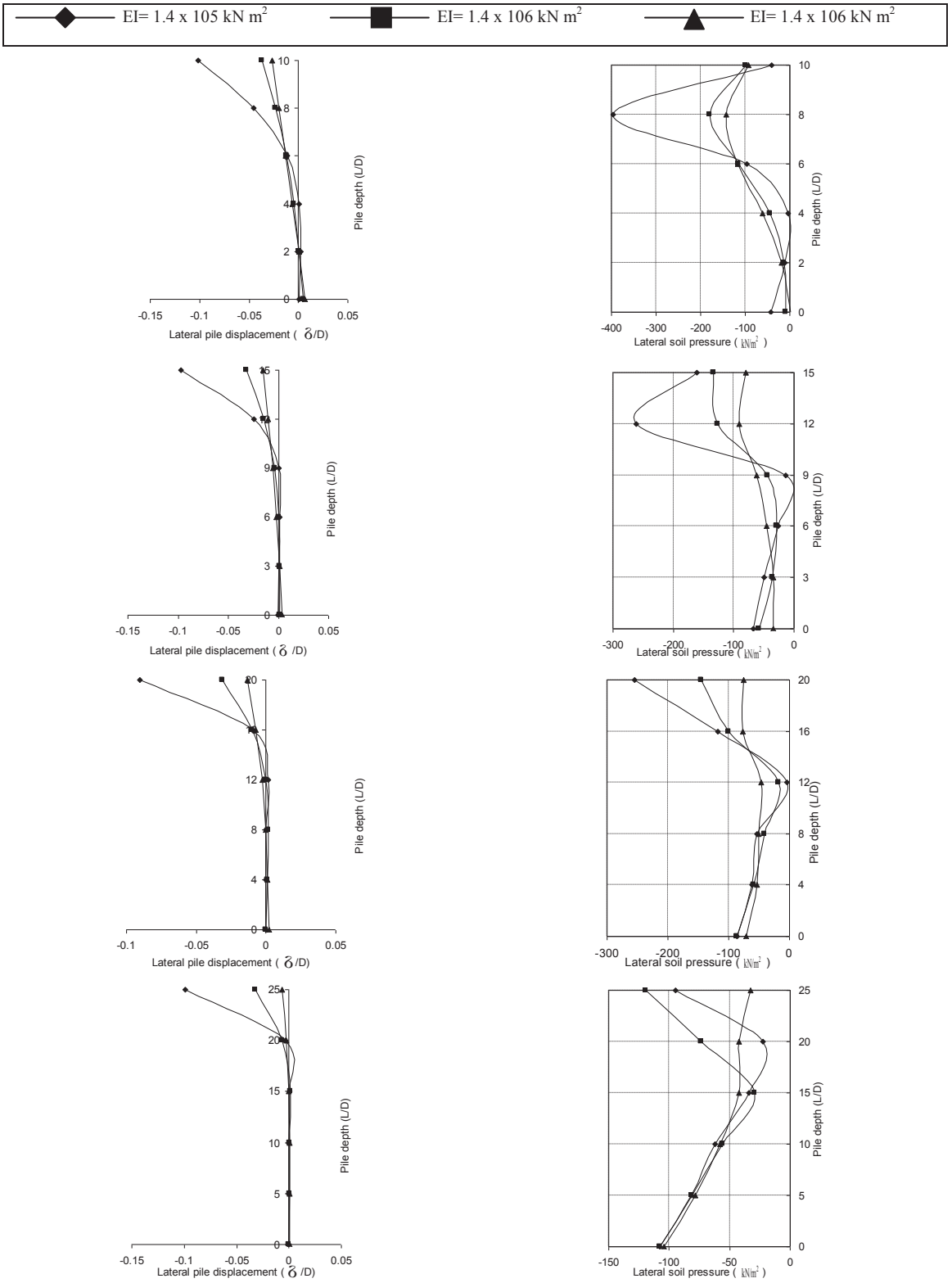

Figure 11: Influence of pile stiffness, *EI*, on the lateral soil pressure for cohesive soil, (a) $L/D = 10$, (b) $L/D = 15$, (c) $L/D = 20$ and (d) $L/D = 25$.

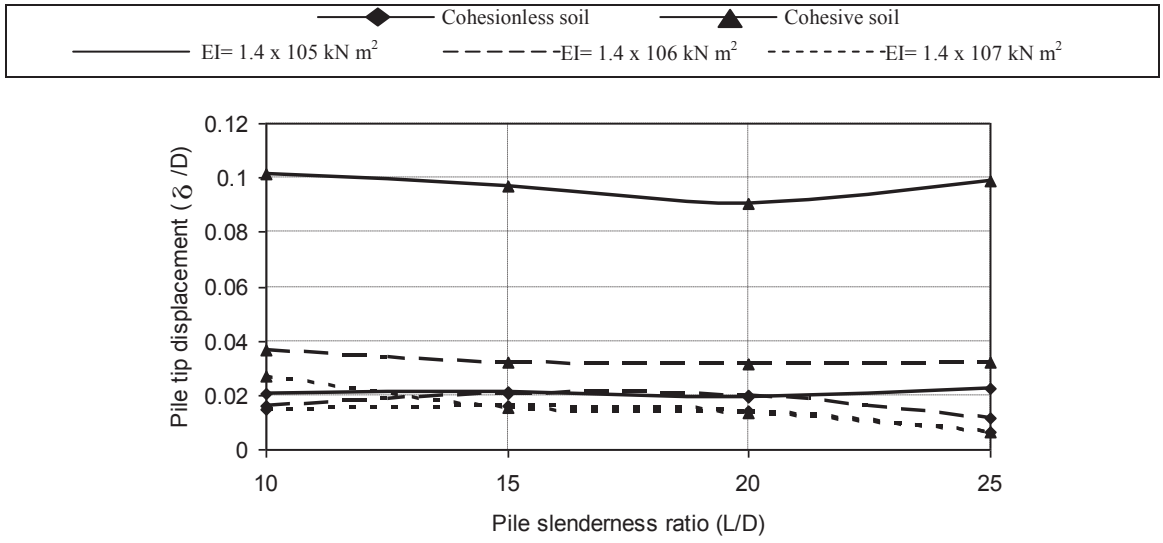

Figure 12: Predicted lateral tip displacement versus pile slenderness ratio under influence of lateral load intensities.

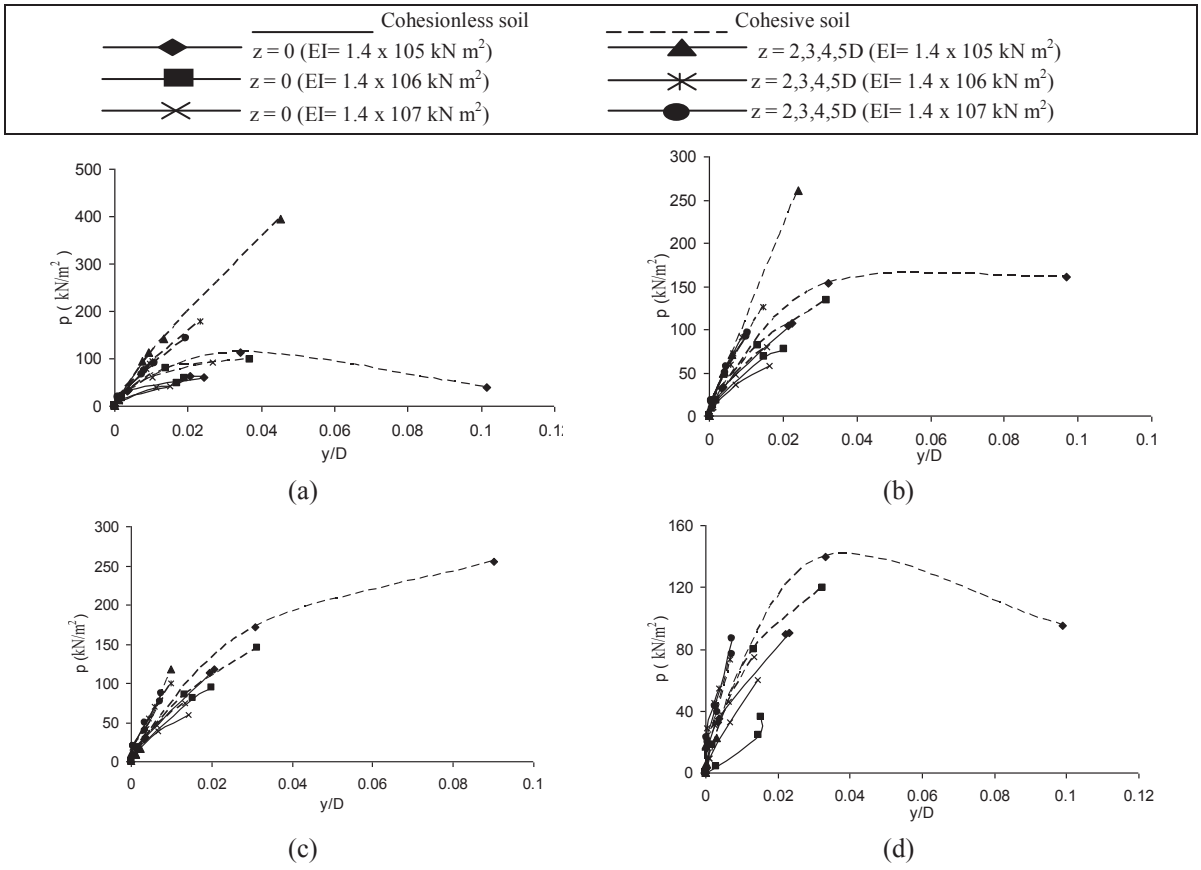

Figure 13: *p–y* curves predicted under the effect of pile stiffness, *EI*, and pile slenderness ratio of pile embedded on both cohesionless and cohesive soils.

The study made comparison of both types of soil under three amounts of *EI*. High lateral tip displacement can be observed in the case of low *EI* of the pile in cohesive soil. This was possibly due to the surrounded soil failure occurred. In addition, it can be observed that low increment in lateral pile displacement appeared in case of cohesionless soil.

The p–y curve predicted from finite element at two depths (z = 0 and z = L/5D) for both cohesionless and cohesive soils is shown in Figure 13. From this figure, it can seem that different behaviour of pile with different *EI* values translates into different design values, if necessary, to design pile under lateral load. Therefore, it can be concluded that the pile is sensitive to the *EI* values as well as a pile slenderness ratio.

5 Conclusion

The lateral pile deformation and lateral soil resistance because of the lateral load is always influenced by the lateral load intensity and soil type as well as a pile slenderness ratio (*L/D*). For the pile of *L/D* = 10, the point of inflection is 1/5 from the base of the pile, whilst the pile with a slenderness ration of *L/D* = 15 and *L/D* = 20, the point position is 1/2 and 3/5 from the base, respectively. Finally, for the pile of *L/D* = 25, the point of inflection (fracture point) is 7/10 from the base. The pile under an intermediate and large amount of loading (in case of cohesionless soil) has more resistance (low lateral displacement) than that embedded on the cohesion soil. The pressure increased with depth. Higher values of pressure were occurred in the position of *L/D* between 6 and 8 when lateral loads of 250 and 450 kN were applied. Non-linear relationship between ultimate lateral soil pressure and the pile slenderness ratio was observed for different load magnitude and soil type.

The square-shaped pile has more resistance compared with a circular pile. The square-shaped pile is able to resist the load by about 30% more than the circular pile. The cross section of square-shaped pile has high amount of lateral soil pressure compared with those observed from the circular pile. Therefore, the p–y design curve is more sensitive to the pile shape as well as a pile slenderness ration. A pile in cohesionless soil was less affected by the change in *EI* compared with that in cohesive soil. The different p–y behaviour of pile with different *EI* values mean different design values, if necessary, to design pile under lateral load. Therefore, the pile is sensitive to the *EI* values as well as pile slenderness ration.

References

[1] Abbas Al-Shamary, J.M., Chik, Z. & Taha, M.R. 2018. Modeling the lateral response of pile groups in cohesionless and cohesive soils. *International Journal of Geo-Engineering*, 9(1), 1-17.

[2] Abbas, J.M., Chik, Z. & Taha, M.R. 2017. Lateral Pile Response Subjected to Different Combination of Loadings. *Journal of Engineering Science and Technology Review* 10 (6), 195- 202

[3] Abbas, J.M., Chik, Z. & Taha, M.R. 2015. Influence of axial load on the lateral pile groups response in cohesionless and cohesive soil. *Front. Struct. Civ. Eng*, 9(2): 176–193.

[4] Anagnostopoulos, C. and M. Georgiadis, 1993. Interaction of axial and lateral pile responses. *J. Geotech. Eng. Division,* 119(4): 793–798.

[5] Brinkgreve, R.B.J. & Broere, W. (2004) "*PLAXIS 3D FOUNDATION - version 1*" Netherlands.

[6] Broms B. B. 1964a . Lateral resistance of Piles in Cohesive Soils . *Journal of the Soil Mechanics and Foundations Division, ASCE*, 90(2): 27-63.

[7] Broms B. B. 1964b . Lateral resistance of Piles in Cohesionless Soils . *Journal of the Soil Mechanics and Foundations Division*, ASCE, 90(3): 123-156.

[8] Davisson, M.T. and Gill, H.L. 1963. Laterally loaded piles in layered soil system. *Journal of Soil Mechanics Foundation Division. ASCE*, 89(3): 63-94.

[9] Johnson, K., Lemcke, P., Karunasena, W., Sivakugan, N. 2006. Modelling the load – deformation response of deep foundation under oblique load. *Environment Modelling and Software*, 21: 1375-1380.

[10] Ismael, N. F. (1998) "Lateral loading tests on bored piles in cemented sands". *Proceedings of the 3rd International Geotechnical Seminar on Deep Foundation on Bored and Auger Piles, Ghent, Belgium* pp.137-144.

[11] Kahyaoglu, M. R., Imancli, G., Ozturk A. U., and Kayalar, A. S. 2009. Computational 3D finite element analyses of model passive piles. *Computational Materials Science*. (In press)

[12] Karthigeyan, S., Ramakrishna, V. V. G. S. T. , and Rajagopal K. 2006 . Influence of vertical load on the lateral response of piles in sand . *Computer and Geotechnics*, 33: 121-131.

[13] Karthigeyan, S., Ramakrishna, V. V. G. S. T. , and Rajagopal K. 2007. Numerical Investigation of the Effect of Vertical Load on the Lateral Response of Piles . *Journal of Geotechnical and Geoenvironmental Engineering*, 133(5): 512-521.

[14] Matlock, H. and Reese, L.C. 1960. Generalized solution for laterally loaded piles. *Journal of Soil Mechanics and Foundations Division*, ASCE, 86, (SM5): 63- 91.

[15] Mroueh, H. and Shahrour, I. 2009. Numerical analysis of the response of battered piles to inclined pullout loads. *International Journal for Numerical and Analytical Methods in Geomechanics*. 33 (10): 1277 – 1288.

[16] Muqtadir, A., and Desai, C. S. 1986. Three-dimensional analysis of a pile-group foundation. *International Journal of Numerical and Analytical Methods Geomechanics* 10: 41–58.

[17] Ooi, P. S.K, Chang, B. K.F. and Wang, S. 2004. Simplified Lateral Load Analyses of Fixed-Head Piles and Pile Groups. *Journal of Geotechnical and Geoenvironmental Engineering,* 130(11): 1140–1151.

[18] Patra, N. R. and Pise, P. J. 2001. Ultimate Lateral Resistance of Pile Groups in Sand, *Journal of Geotechnical and Geoenvironmental Engineering,* 127(6): 481-487.
[19] Pise, P. J. 1982. laterally loaded piles in a two-layer soil system. *Journal of Geotechnical Engineering,* 108(9): 1177-1181.
[20] Poulos H. G., and Davis E. H. 1980 . *Pile Foundation Analysis and Design* . John Wiley & Sons, New York.
[21] Potts, D. M., and Zdravkovic, L. 1999. Finite element analysis in geotechnical engineering: theory. Thomas Telford. Heron Quay, London.
[22] Reese, L.C. & W.F. Van Impe 2011. Single Piles and Pile Groups Under Lateral Loading, 2nd Edition. London: Taylor & Francis Group.
[23] Trochanis, A. M., Bielak, J. and Christiano, P. 1991. Three-dimensional nonlinear study of piles. *Journal of Geotechnical Engineering*, ASCE, 117(3): 429.447.
[24] Yang Z. and Jeremic B. 2002 . Numerical Analysis of Pile Behavior under Lateral Loads in Layered Elastic-Plastic Soils . *International Journal for Numerical and Analytical Methods in Geomechanic*s, Vol 26, 1385–1406.
[25] Zhang, L., F. Silva and R. Grismala, 2005. Ultimate lateral resistance to pile in cohesionless soils. *J. Geotech. Geoenvir. Eng. ASCE*., 131(1): 78-83